

# Simultaneous Production of Bioethanol and Bioelectricity in a Membrane Less Single Chambered Yeast Fuel Cell by *Saccharomyces Cerevisiae* and *Pichia Fermentans*

**Akansha Shrivastava**

Manipal University Jaipur

**Mamta Pal**

Manipal University Jaipur

**Rakesh Kumar Sharma** (✉ [rakeshkumar.sharma@jaipur.manipal.edu](mailto:rakeshkumar.sharma@jaipur.manipal.edu))

Manipal University Jaipur <https://orcid.org/0000-0002-2826-1291>

---

## Research

**Keywords:** Pichia fermentans, Saccharomyces cerevisiae, Single chambered MFC, Ethanol production, Columbic efficiency

**Posted Date:** April 19th, 2021

**DOI:** <https://doi.org/10.21203/rs.3.rs-405049/v1>

**License:** © ⓘ This work is licensed under a Creative Commons Attribution 4.0 International License.

[Read Full License](#)

---

# Abstract

Production of bioethanol and bioelectricity is a promising approach through microbial electrochemical technology. Sugars are metabolized by yeast to produce ethanol, CO<sub>2</sub> and energy. Surplus electrons produced during the fermentation can be transferred through the circuit to generate electricity in a Microbial fuel cell (MFC). In the present study, a membrane less single chambered microbial fuel cell was developed for simultaneous production of bioethanol and bioelectricity. *Pichia fermentans* along with a well-known ethanol producing yeast *Saccharomyces cerevisiae* was allowed to ferment glucose. *S. cerevisiae* demonstrated maximum open circuit voltage (OCV)  $0.287 \pm 0.009$  V and power density  $4.473 \text{ mW m}^{-2}$  on 15th day, with a maximum ethanol yield of 5.6% (v/v) on 12th day. *P. fermentans* demonstrated a maximum OCV of  $0.318 \pm 0.0039$  V and power density of  $8.299 \text{ mW m}^{-2}$  on 15th day with ethanol yield of 4.7 % (v/v) on 12th day. Coulombic efficiency (CE) increased gradually from 0.002–0.471 % and 0.012–0.089 % in the case of *S. cerevisiae* and *P. fermentans*, respectively, during 15 days of experiment. Thus, the result indicated that Single chambered fuel cell can be explored for its potential applications for ethanol production along with clean energy generation.

## 1. Introduction

Fossil fuels are naturally occurring carbon or hydrocarbon fuel such as peat and coal while natural gases are formed by the decay of plants or animals. The products formed by fossil fuels are essential for our living and required for the production of materials like plastics, medicines, life-saving devices, gasoline, fuel, heating oil, while natural gas to be used as fuel and generate electricity. In spite of being several usages, increasing price and negative environmental impact of fossil fuels have increased the concerns related to its future availability and use. Several potential alternative fuels including biodiesel, methanol, hydrogen, natural gas, bio-oil, bio-char, liquefied petroleum gas (LPG), Fischer–Tropsch fuel, p-series, bioelectricity, and solar fuels (Aditya et al. 2016; Baig et al. 2019) have been developed. Moreover, bioethanol is also produced from various agricultural raw materials such as sucrose-containing feedstocks, lignocellulosic materials and starch materials (Bušić et al. 2018). Since the conversion of lignocellulosic biomass into ethanol is difficult due to the fact of being resistant in nature to be degraded (Liu et al. 2019). Bioethanol is a promising liquid fuel that is expected to have promising future.

The increasing interest in bioethanol production started since 1980s and hence has been considered as an alternative fuel in many countries. It helps to reduce CO<sub>2</sub> emission up to 80% as compared to using the petrol, thus encourages a healthier environment for the future. They are recyclable and contribute to sustainability. Similarly, production of bioelectricity in microbial fuel cell (MFC) as biotechnological system is another developing green approach towards renewable energy from sustainable development (Paul et al. 2018; Kumar et al. 2019). Bioelectricity is produced through microbial catalytic activity using various organic sources. In MFC, anode accepts electrons from microbial catabolic activity through oxidation and reduction processes. In general, it is evident that 2 mol of ethanol is produced from 1 mol of glucose (glucose → Pyruvate → acetaldehyde → ethanol) through NADH-dependant enzyme and

alcohol dehydrogenase. This reaction generates two ATP molecules, two H<sup>+</sup> ions and two electrons. These electrons are stored in cells in the form of NADH. An increasing ratio of NADH to NAD<sup>+</sup> could help to generate voltage output (Geng et al. 2020). Thus the generated electrons from NADH/NAD<sup>+</sup> redox cycle may be used in MFC system (Walker and Stewart 2016). Therefore, it is possible that yeast metabolic activity, energy production and its conversion into heat could be efficiently harvested as electricity through a combined approach of MFC during sugar fermentation and ethanol production.

Yeast could potentially be considered as an ideal model organism for MFC applications due to its non-pathogenic nature and being able to utilize a wide-ranging substrate. The most commonly used biocatalyst for fermenting the sugars into ethanol is *Saccharomyces cerevisiae*, but its use is restricted as it cannot ferment xylose and other 5-carbon sugars present in lignocellulosic material. On the other hand, xylose-fermenting yeasts e.g. *Pichia stipitis*, *Candida parapsilosis* and *Candida shehatae* (Mohd Azhar et al. 2017) may ferment both 5-carbon as well as 6-carbon sugars. *Pichia fermentans* has also been reported to produce xylitol using non-detoxified xylose rich pre-hydrolysate from sugarcane bagasse (Prabhu et al. 2020).

Recently published reports suggests that non-pathogenic *Pichia fermentans* could be a potential yeast to be used in a microbial fuel cell due to its possible exoelectrogenic property (Pal and Sharma 2019). The signaling molecule produced by one cell and sensed by another to induce oriented growth is considered for cell-cell communication (Stephens and Bentley 2020). Most bacterial communities are embedded in structured extracellular polymeric substances (EPS) to survive in a harsh environment (Flemming and Wuertz 2019). Electroactive biofilms play an important role in bioelectrochemical system via various electron transfer mechanism. Yeasts may also produce biofilm to enhance electron transfer mechanism and biofilm dynamics in microbial fuel cells (Speranza et al. 2020).

Most of the work related to MFC has been focused on reactor design, proton exchange membrane, electrolyte development and modification of electrode design and materials to increase electricity production (Christwardana et al. 2019). There are several advantages in MFC as it can be operated in fed batch, continuous or batch mode whether single chambered or double chambered, with membrane or membrane less etc. This paper presents an approach to explore MFC for bioethanol production with simultaneous generation of electricity. The study further evaluates the production of ethanol in MFC by *P. fermentans* and compared its efficiency with a well-known sugar fermenting yeast *S. cerevisiae* under a batch type operation in a single chambered Microbial fuel cell. The electrochemical data was generated by calculating current density, power density, output voltage along with the glucose consumption for maximum ethanol yield and fermentation efficiency.

## 2. Experimental Section

### 2.1 Microorganisms

*Pichia fermentans* was procured from the Microbial Type Culture collection (MTCC 189) Chandigarh, India, and cultured aerobically in yeast extract and glucose (YG) agar and maintained. And *Saccharomyces cerevisiae* was purchased from local market and maintained. Both the yeasts, *P. fermentans* and *S. cerevisiae* was cultured for 24 hours at 30°C enriched with yeast extract 0.25% (w/v) and Glucose 10% (w/v) in a 1L solution. The same broth medium was used for inoculum preparation to be inoculated in the MFC.

## 2.2 Single Chambered MFC setup

A typical mediator less membrane less single chambered MFC was constructed using glass flasks (with working volume 100 mL). Bow shaped Carbon fibers (100 cm length, 7 mm diameter) were used as anode and circular stainless steel wire (as a mesh) (100 cm length, 0.05 mm diameter) as cathode (Nam et al. 2018). Both the electrodes were sterilized with ethanol, rinsed with autoclaved distilled water, and treated under UV radiation for 20 min, then dried under aseptic conditions. The flasks contained production medium (Glucose 10% (w/v), enriched with yeast extract 0.25% (w/v) was sterilized and then sterilized electrodes were fixed at a vertical distance of 3 cm using rubber corks as plug to maintain anaerobic condition for fermentation. The flasks were inoculated with either of the yeast (10 % (v/v) and incubated at 30°C for 15 days. All experiments were performed in triplicates and repeated along with suitable controls. The sample (2 ml) was taken out for glucose and ethanol estimations.

## 2.3 Electrochemical calculations

The open circuit voltage (OCV) and output voltage was recorded across different external resistor ranging from 1000Ω to 820KΩ via a digital multimeter. For the preparation of polarization curve the external resistance ( $R_{ex}$ ) was varied at time intervals. The current ( $I$ ) was calculated by using Ohm's law  $V = IR$ , where  $V$  represents cell voltage value and  $R$  represents external resistance value. Power was calculated according to  $P = VR$  whereas, Current density ( $j$ ) and power density ( $p$ ) were calculated using electrode (anode) area ( $2.2 \text{ cm}^2$ ). The Coulombic efficiency (CE) was calculated using  $CE = CE_x \times 100 / C_{TH}$ ,  $CE_x$  is the experimental value of total coulombs. The theoretical value of coulombs ( $C_{TH}$ ) was calculated using  $C_{TH} = FnMV$ , where  $F$  stands for faraday constant (96,485C per mole of electrons),  $n$  represents number of electrons produced per glucose unit consumed during fermentation,  $M$  is the glucose concentration and  $V$  represents the reaction volume (L). Internal resistance ( $R_{int}$ ) of the cell was calculated as  $R_{int} = R (E/V-1)$  where  $R$  represents external resistance,  $E$  represents OCV (voltage without any resistance), and  $V$  represents output voltage with resistors (Pal and Sharma 2020). All data presented in the manuscript are average of triplicates along with the standard error bars.

## 2.4 Glucose estimation

Concentration of glucose in the cell setup was routinely measured by dinitrosalicylic acid (DNS) method. The quantification was performed according to the step-by-step method (Pal and Sharma 2019). DNSA reagent was prepared by dissolving 2g of DNSA and 60g of sodium-potassium tartaric acid in 160 mL of 0.5N NaOH. It was cooled to room temperature and diluted to 200mL with the help of distilled water. Then 1 mL of DNSA reagent was pipette out in a test tube containing 0.5 mL of sample (1g/mL) and kept at

100°C for 5 min. After cooling, 1.5 mL of distilled water was added to the same test tube to stop further reaction and absorbance was measured at 540 nm using UV-VIS spectrophotometer. The glucose concentration was calculated from the standard curve of D-glucose (0.1mg-1g/mL), and results were expressed as mg glucose equivalent (GE) per mL sample. The ethanol fermentation was confirmed by using High performance liquid chromatography.

## 2.5 Ethanol estimation

All parameters were performed with an Agilent HPLC 1260 II INFINITY with autosampler and C18 column (5 µm; 25 x 0.46cm). All the outputs were processed through Agilent Chemstation-Open lab software. All samples were drawn out and recorded on daily basis. The sample was centrifuged at 8000 rpm for 15 min to collect for further process. The total runtime was 6 min with peaks detected with a UV detector. Water was used as a mobile phase with 4% acetone added in an optimized parameter. The standard flow rate was set at 1mL/min with injection volume of 1µL and detection was monitored at 235 nm and 25°C temperature. Standard ethanol solutions were prepared in water ranging from 0.1% -10% (v/v).

Ethanol absorbs less UV compared to high UV absorbing background, which result in the reverse positive or negative peak polarity. Direct estimation of ethanol as a negative peak from samples was confirmed by reversed phase-HPLC and performed same according to (Nisha et al. 2016). In every run, the three peaks were corresponding to acetone, ethanol or water singly or in combination were detected. Acetone, pure water and ethanol samples were injected separately for separate verification of retention times into the HPLC system in separate runs. The quantitative analysis of ethanol was calculated from the formula-

Concentration of unknown sample = Unknown sample area / standard solution area × concentration of standard solution

Where peak areas are in arbitrary units and peak heights and area in milli absorbance units (mAU).

## 2.6 EPS production

*P. fermentans* and *S. cerevisiae* were grown separately in 10mL sterilized Yeast extract and Glucose (YG) broth and incubated for 15 days at 30°C. The samples were taken out from both the cultures at altered time intervals (day 1, day 5, 10 and 15) to estimate EPS. Ten mL of cell culture was centrifuged simultaneously at 8000 rpm for 15 min. The carbohydrate in EPS was analysed by phenol/sulphuric acid method and glucose was used as a standard (Pal and Sharma 2019). Protein was estimated by Lowry method and bovine serum albumin was used as a standard (Zhang et al. 2019).

## 2.7 Fourier transform infrared spectroscopy

Functional groups in EPS were detected by Fourier transform infrared (FTIR) spectroscopy. A drop of EPS solution from both the samples was used for study on a glass slide as a dry film.

## 2.8 Scanning electron microscopy

The visual appearance of *P. fermentans* and *S. cerevisiae* was evaluated on anodic surface at 1000X magnification. The sample was prepared by using electrode material from both the cell cultures at different time interval (day 1, 5, 10 and 15) and was air dried on a glass slide.

## 3. Results & Discussion

### 3.1 Performance of MFC

Combination of fermentation and electricity generation demonstrated a promising performance in the MFC. Both the yeast *S. cerevisiae* and *P. fermentans* grew rapidly under experimental setup (membrane less single chambered MFC). All the setup depicted a typical behaviour of MFC in terms of its electrochemical responses. In the absence of exogenous electron mediator, the intracellular proteins of the model organisms play a major role in electron transfer located inside the cell. This could possibly overcome by adherence of yeast cells to the carbon fibre surface through force driven interaction such as electrostatic or physical adsorption (Rossi et al. 2015).

### 3.2 Electrochemical response

Electrochemical performance of both the MFC setup containing either *P. fermentans* or *S. cerevisiae*, gradually increased after 24 h of inoculation, which was almost stable upto 15 days of the incubation. Maximum OCV for *P. fermentans*  $0.318 \pm 0.0039$  V was recorded on 15th day (Fig. 1a).

Current density also increased gradually from  $4.848 \text{ mA m}^{-2}$  (1st day) to  $57.348 \text{ mA m}^{-2}$  (15th day) (Fig. 2c and d). Power density of the cell also followed similar pattern with maximum power density of  $8.299 \text{ mW m}^{-2}$  was recorded on 15th day. For *S. cerevisiae* maximum recorded OCV was  $0.287 \pm 0.009$  V on 15th day (Fig. 1a) with increasing current density from  $1.66 \text{ mA m}^{-2}$  on 1st day to  $43.63 \text{ mA m}^{-2}$  on 15th day (Fig. 2a and b). Power density was also recorded with same increasing pattern out of which maximum is  $4.47 \text{ mW m}^{-2}$  on 15th day (Fig. 2a).

The internal resistance ( $R_{\text{int}}$ ) was very high against different  $R_{\text{ex}}$  from  $1000 \Omega$ - $82 \text{ K}\Omega$  for both the organisms on 1st day which drastically decreases from 2nd day onwards (Fig. 3a and b). Combination of carbon fibre anode and stainless steel cathode has been explored well in the setup. Thus indicates the present setup was intact without any physical damage or corrosion and can be reused efficiently after sterilization. MFC appears to be an ecological approach to achieve the cost-effective electricity generation. The maximum power density for *P. fermentans* was  $8.299 \text{ mW m}^{-2}/100\text{mL}$  while the current density was  $57.348 \text{ mA m}^{-2}/100\text{mL}$  on 15th day and  $0.318 \pm 0.0039$  V power output for the same day. From past years, *Pichia* has been explored in the field of MFC such as *Pichia pastoris*, *Pichia stipitis*, *Pichia kudriavzevii* etc., for power generation with genetic modifications and less interest was focused on efficient bioethanol formation (Pal and Sharma 2019). Whereas the *S. cerevisiae* was measured at power density of  $4.473 \text{ mW m}^{-2}/100\text{mL}$  on 15th day while the current density was  $43.636 \text{ mA m}^{-2}/100\text{mL}$  on 15th day and power output was of  $0.287 \pm 0.0094$  V.

Amongst them *P. fermentans* was resulted in better power, current density and OCV than *S. cerevisiae*. This is because of low resistance and large surface area of carbon brush electrode. Makes them ideal features as anodes from small as well as large scale applications of MFCs (Yuan et al. 2020a). Yuan et al recently published a report on simultaneous power generation system and bioethanol formation. In this, they used *S. cerevisiae* as model organism for dual and single chambered MFC setup with or without Mediator for power generation and ethanol production. This study resulted in a high power output ( $5.2 \pm 0.5 \text{ W/m}^3$ ) and high ethanol yield ( $92.5 \pm 2\%$ ). There are many factors affecting electron transport such as cell metabolism, pH value, mediator type, yeast cell growth, substrate. But excessive addition of MB for electron transfer could affect the activity of yeast and lasts in unbalancing and blocking of electron transmission.

### 3.3 Glucose consumption and ethanol production

The quantifiable reducing sugar content was carried out using Dinitrosalicylic acid (DNSA) method. Basic principle involves for the method is interaction of an alkaline solution of DNSA with reducing sugars such as glucose and fructose wherein the aldehyde group of reducing sugar is oxidized to the carboxylic acid and the 3-nitro group ( $\text{NOO}^-$ ). The change in colour was measured at 540 nm (Jain et al. 2020). The variation of the orange-red color index was the indication of presence of reducing sugar to high/low extent.

The sugar consumption and ethanol production by these yeasts was studied in 100 mL single chambered cell setup in sugar medium containing 10% (Glucose) 100 mL Erlenmeyer flasks, supplemented with 0.25% yeast extract and incubated as described above. The glucose content was calculated from the standardization curve of D-glucose ( $y = 6.5333x + 0.0613$ ,  $R^2 = 0.9909$ ) and expressed as mg/mL. The glucose was efficiently consumed during initial days of incubation period; about 15–20% of glucose was consumed in one day. After 24 h, the glucose concentration reduced from 10% (w/v) to  $7.8 \pm 0.0004\%$  (w/v) in the reactors inoculated with *P. fermentans* and  $8.4 \pm 0.0003\%$  (w/v) for *S. cerevisiae*, while the glucose concentration was only  $0.2 \pm 0.00002\%$  (w/v) at the end of the experiment. A detectable amount 0.025% (v/v) of ethanol was observed on day 1 for *P. fermentans*, which was maximum on 12th day 4.7% (v/v) and remain constant on 13th day and decreased gradually. As, *Pichia* utilizes hexoses slowly than pentose sugar as a carbon source and ethanol formation during fermentation process (Tahir and Mezeri 2020).

Whereas, in the case of *S. cerevisiae* the ethanol concentration measured on day 1 was 0.03 % (v/v) with remaining glucose concentration of 8.4 % (w/v). *S. cerevisiae* produced maximum ethanol on 12th day 5.6 % (v/v) and the remaining glucose concentration was left with 0.23 % (w/v) at the end of experiment (Fig. 4a and b). It shows alcohol production by yeast cells *P. fermentans* and *S. cerevisiae* on day wise fermentation analysis.

The 24 h old cells subjected to fermentation in a 10 % glucose solution (10g/100mL) and have ability to ferment glucose to ethanol. The cell setup of *P. fermentans* showed maximum 4.7 % (v/v) ethanol production of theoretical yield (6.41 % v/v for 10 % glucose) on day 12 and continued to remain constant

upto day 13 and gradually decreased on consecutive days (Nandal et al. 2020). Since 1 mol of glucose produces 2 mol of ethanol and  $2\text{CO}_2$ . This infers that the power generation in MFC setup is independent of fermentation process. In point of fact, ethanol and power generation occur concurrently with the process of glucose metabolization through yeast. It been reported from several studies that under anaerobic conditions, 1 mol of glucose can be converted to give 2 mol of ethanol and 2 mol of electrons. It is evident that the under anaerobic conditions, yeast-MFC cannot utilize all the electrons from complete oxidation of glucose. Another major reason is the direct electron transfer by a yeast cell is very limited, as compared to *Shewanella* and *Geobacter* (Christwardana et al. 2018). Therefore, this study focused on the simultaneous production of both bioethanol and electricity generation so that the substrate can be fully utilized for significant benefit.

Based on the stoichiometric information, glucose concentrations were theoretically converted to electron amounts. It was used to calculate the amount of electrons passed through the MFC circuit during glucose oxidation (Flimban et al. 2019). The CE According to the formula for CE,  $\text{CE} = (\text{CE}_x \times 100 / \text{C}_{\text{Th}})$ , one can calculate how many electrons were involved in electron transfer through the MFC external circuit (Yuan et al. 2020b). Over 24 h, the CE of the proposed MFC setup for *P. fermentans* was 0.012% and increased upto 0.89% gradually along with the increase in the current density (Fig. 1b). Whereas, the CE efficiency after 24 h for the *S. cerevisiae* was 0.002% and increased to 0.47% on concluded day. Still, most of the electrons may possibly involve in the ethanol production process. This indicates that MFC setup had little effect on fermentation efficiency (Walker and Stewart 2016; Yuan et al. 2020a). The carbon fibre of electrode provides massive surface area for yeast adsorption on its electrode surface. Hence, the application of yeast cells on carbon fibre electrode improved the immobilization effect onto the electrode (Yuan et al. 2020a). A higher glucose concentration would yield more electrons for high electricity generation and ethanol (dos Passos et al. 2019; Zhao and Zhang 2019). Whereas, a massive literature survey suggests the ongoing efforts for energy generation and biofuel formation (Moradian et al. 2021). Still there is lot to unravel about the efficient mechanism behind the electron transfer and different substrates conversion to energy generation requires further consideration.

### 3.4 Effect of pH

In industrial ethanol production, yeast tolerates wide range of pH, thus making the whole process less susceptible to contamination. It was observed that higher acidic conditions produces larger amount of ethanol (Mohd Azhar et al. 2017). At the time of yeast fuel cell setup for *P. fermentans* and *S. cerevisiae*, the initial pH was maintained at 7. In the cells inoculated with *P. fermentans*, the pH decreases to 6.5 after 24 h and here ethanol was measured is 0.3% (v/v), which was further decreased to 5 and was constant from day 4 to day 7 and during these days the concentration of ethanol ranged from 0.8–2.3% (v/v). A decrease in pH and increase in ethanol yield was observed during further incubation. In *S. cerevisiae* after 24 h the pH decreased upto 6.6 and a detectable volume of ethanol was recorded 0.3% (v/v). The pH decreased upto 5 during further 9 days of incubation and increasing ethanol concentration upto 5.6% (v/v). As per the results obtained *P. fermentans* produced maximum ethanol 4.7% on 12th day with pH 4.3, while *S. cerevisiae* produced maximum ethanol 5.6% on 12th day of incubation with 4.8 pH (Figure

S1). The yeast *S. cerevisiae* strains are considered to be pillars of fermentation industry since then dominated ethanol fermentation due to their low pH tolerance for ethanol formation, organic acids, and low oxygen availability. It is evident that in *P. fermentans* the correlated effect of respiratory and fermentative pathways supports growth and product formation. This yeast ferments glucose or xylose under oxygen-limited conditions (Kwak et al. 2019).

## 3.5 EPS production

EPS production was observed in both the yeast *P. fermentans* and *S. cerevisiae* along with their growth and colonization on anode surface. Growing biofilm were observed under scanning electron microscopic images (Fig. 5).

The biofilm was developed on the anode surface as well as on the top of the medium. A significant correlation between EPS production and yeast growth was observed as analysed on different days (day 1, 5, 10 and 15). The cells grew rapidly along with the biomass accumulation on different time intervals and resulted in gradual increase in biomass, protein, EPS and carbohydrate (Fig. 6a and b).

Both the yeast *P. fermentans* and *S. cerevisiae* produced EPS along with a dense biofilm on carbon fibre anode, which showed efficient direct electron transfer. However, its EPS may have boosted the electron transfer via the indirect mechanism (Pal and Sharma 2019). Evident studies suggested that the combination of yeast attached anode improves electron transfer directly creating synergistic effect (Chung et al. 2016). EPS composed of polysaccharides, extracellular DNA, glycoproteins, glycolipids and proteins. This EPS plays some significant roles such as microbial cell to cell communication, protection from external and specially extracellular electron transfer (Flemming et al. 2016). It is evident that presence of carbohydrate in EPS carry out specific functions in mat formation.

The protective glycocalyx acts as a mediator in yeast for electron transfer and may be involved in oxidation and reduction reactions. The presence of EPS matrix was confirmed by infrared (IR) spectrum. After 24 h (day 1), the EPS production for *Saccharomyces cerevisiae* and *Pichia fermentans* was minimum but increased gradually during further incubation on day 5, day 10 and day 15. The spectrum of purified EPS showed numerous peaks from 3585 – 502  $\text{cm}^{-1}$  (Figure S2a and b). The EPS absorption frequency from 3585 to 3174  $\text{cm}^{-1}$  and 3688 – 3071  $\text{cm}^{-1}$  showed the presence of alcoholic (O-H) group, primary and secondary amine group confirms the polysaccharide nature of EPS produced by *S. cerevisiae* and *P. fermentans*, respectively. Peaks ranging from 2969 – 2763  $\text{cm}^{-1}$  and 2956 – 2763  $\text{cm}^{-1}$  represent saturated aliphatic (alkene/alkyl) with methyl C-H ( $-\text{CH}_3$ ) asymmetrical/symmetrical stretch and ether and oxy compound with methoxy, C-H stretch ( $\text{CH}_3\text{-O-}$ ) in the case of *S. cerevisiae* and *P. fermentans*, respectively (Abid et al. 2021). The absorption peak at 1628  $\text{cm}^{-1}$  was due to the stretch vibration of carboxyl group ( $\text{C}=\text{O}$ ) in *S. cerevisiae*. Peaks ranging from 1838 – 1221  $\text{cm}^{-1}$  represents primary amide  $\text{C}=\text{O}$ ,  $-\text{CONH}_2$  and secondary amide with N-H stretch bend in EPS produced by *P. fermentans*.

The absorption peaks ranging from 1011 to 1036  $\text{cm}^{-1}$  showed alkyl halide and stretching vibrations of pyranose ring (Li et al. 2014). The peaks between 904 – 509 & 604  $\text{cm}^{-1}$  showed stretch of alkyl halides

and d (C-O-C) glycosidic linkage respectively (Pal and Sharma 2019).

## 4. Conclusion

In this study a system for simultaneous power generation and ethanol production was developed. The study demonstrated ethanol production by *Pichia fermentans* and *Saccharomyces cerevisiae*, which reached upto 4.7% and 5.6% v/v of the theoretical yield (6.41% (v/v)) respectively for 10% glucose in yeast microbial fuel cell. Analysis of EPS showed the presence of polysaccharides, protein having several functional groups like C = O, -CONH<sub>2</sub>, -CH<sub>3</sub> and OH, of *P. fermentans* and *S. cerevisiae*. Another important aspect of the present study is the application of *P. fermentans* for ethanol production in a fuel cell, which was not explored yet. *P. fermentans* turned out as an efficient yeast for further microbial fuel cell application.

## Declarations

Ethics approval and consent to participate: Not Applicable

Consent for publication: Yes

Availability of data and materials: Not Applicable

Competing interests: Not Applicable

Funding: Not Applicable

Authors' contributions: AS performed the experimental work, analyses of data and prepared draft of the manuscript. MP analysed the data, and writing of manuscript. RKS conceptualized and supervised the work, and edited the manuscript.

Acknowledgements: Authors acknowledge Manipal University Jaipur for providing SEM and HPLC facilities.

Authors' information: AS and MP hold M Sc in Microbiology and working as Ph D research scholars. RKS is an Assistant Professor in the Department of Biosciences, Manipal University Jaipur and supervising their Ph D.

## References

1. Abid Y, Azabou S, Blecker C et al (2021) Rheological and emulsifying properties of an exopolysaccharide produced by potential probiotic *Leuconostoc citreum*-BMS strain. Carbohydr Polym 256:117523. <https://doi.org/https://doi.org/10.1016/j.carbpol.2020.117523>
2. Aditya HB, Mahlia TMI, Chong WT et al (2016) Second generation bioethanol production: A critical review. Renew Sustain Energy Rev 66:631–653. <https://doi.org/10.1016/j.rser.2016.07.015>

3. Baig KS, Wu J, Turcotte G (2019) Future prospects of delignification pretreatments for the lignocellulosic materials to produce second generation bioethanol. *Int J Energy Res* 43:1411–1427. <https://doi.org/https://doi.org/10.1002/er.4292>
4. Bušić A, Mardetko N, Kundas S et al (2018) Bioethanol production from renewable raw materials and its separation and purification: A review. *Food Technol Biotechnol* 56:289–311. <https://doi.org/10.17113/ftb.56.03.18.5546>
5. Christwardana M, Frattini D, Accardo G et al (2018) Optimization of glucose concentration and glucose/yeast ratio in yeast microbial fuel cell using response surface methodology approach. *J Power Sources* 402:402–412. <https://doi.org/10.1016/j.jpowsour.2018.09.068>
6. Christwardana M, Frattini D, Duarte KDZ et al (2019) Carbon felt molecular modification and biofilm augmentation via quorum sensing approach in yeast-based microbial fuel cells. *Appl Energy* 238:239–248. <https://doi.org/10.1016/j.apenergy.2019.01.078>
7. Chung Y, Ahn Y, Christwardana M et al (2016) Development of a glucose oxidase-based biocatalyst adopting both physical entrapment and crosslinking, and its use in biofuel cells. *Nanoscale* 8:9201–9210. <https://doi.org/10.1039/c6nr00902f>
8. dos Passos VF, Marcilio R, Aquino-Neto S et al (2019) Hydrogen and electrical energy co-generation by a cooperative fermentation system comprising *Clostridium* and microbial fuel cell inoculated with port drainage sediment. *Bioresour Technol* 277:94–103. <https://doi.org/https://doi.org/10.1016/j.biortech.2019.01.031>
9. Flemming HC, Wingender J, Szewzyk U et al (2016) Biofilms: An emergent form of bacterial life. *Nat Rev Microbiol* 14:563–575. <https://doi.org/10.1038/nrmicro.2016.94>
10. Flemming HC, Wuertz S (2019) Bacteria and archaea on Earth and their abundance in biofilms. *Nat Rev Microbiol* 17:247–260. <https://doi.org/10.1038/s41579-019-0158-9>
11. Flimban SGA, Ismail IMI, Kim T, Oh SE (2019) Overview of recent advancements in the microbial fuel cell from fundamentals to applications: Design, major elements, and scalability. *Energies* 12:3390. <https://doi.org/10.3390/en12173390>
12. Geng BY, Cao LY, Li F et al (2020) Potential of *Zymomonas mobilis* as an electricity producer in ethanol production. *Biotechnol Biofuels* 13:. <https://doi.org/10.1186/s13068-020-01672-5>
13. Jain A, Jain R, Jain S (2020) Quantitative Analysis of Reducing Sugars by 3, 5-Dinitrosalicylic Acid (DNSA Method). pp 181–183. [https://doi.org/10.1007/978-1-4939-9861-6\\_43](https://doi.org/10.1007/978-1-4939-9861-6_43)
14. Kumar SS, Kumar V, Malyan SK et al (2019) Microbial fuel cells (MFCs) for bioelectrochemical treatment of different wastewater streams. *Fuel* 254:115526. <https://doi.org/https://doi.org/10.1016/j.fuel.2019.05.109>
15. Kwak S, Jo JH, Yun EJ et al (2019) Production of biofuels and chemicals from xylose using native and engineered yeast strains. *Biotechnol Adv* 37:271–283. <https://doi.org/https://doi.org/10.1016/j.biotechadv.2018.12.003>
16. Li W, Ji J, Chen X et al (2014) Structural elucidation and antioxidant activities of exopolysaccharides from *Lactobacillus helveticus* MB2-1. *Carbohydr Polym* 102:351–359.

<https://doi.org/10.1016/j.carbpol.2013.11.053>

17. Liu CG, Xiao Y, Xia XX et al (2019) Cellulosic ethanol production: Progress, challenges and strategies for solutions. *Biotechnol Adv* 37:491–504. <https://doi.org/10.1016/j.biotechadv.2019.03.002>
18. Mohd Azhar SH, Abdulla R, Jambo SA et al (2017) Yeasts in sustainable bioethanol production: A review. *Biochem Biophys Reports* 10:52–61. <https://doi.org/10.1016/j.bbrep.2017.03.003>
19. Moradian JM, Fang Z, Yong Y-C (2021) Recent advances on biomass-fueled microbial fuel cell. *Bioresour Bioprocess* 8:14. <https://doi.org/10.1186/s40643-021-00365-7>
20. Nam T, Son S, Kim E et al (2018) Improved structures of stainless steel current collector increase power generation of microbial fuel cells by decreasing cathodic charge transfer impedance. *Environ Eng Res* 23:383–389. <https://doi.org/10.4491/eer.2017.171>
21. Nandal P, Sharma S, Arora A (2020) Bioprospecting non-conventional yeasts for ethanol production from rice straw hydrolysate and their inhibitor tolerance. *Renew Energy* 147:1694–1703. <https://doi.org/10.1016/j.renene.2019.09.067>
22. Nisha M, Shankar M, Krishnan N et al (2016) Direct estimation of ethanol as a negative peak from alcoholic beverages and fermentation broths by reversed phase-HPLC. *Anal Methods* 8:4762–4770. <https://doi.org/10.1039/c6ay01075j>
23. Pal M, Sharma RK (2019) Exoelectrogenic response of *Pichia fermentans* influenced by mediator and reactor design. *J Biosci Bioeng* 127:714–720. <https://doi.org/10.1016/j.jbiosc.2018.11.004>
24. Pal M, Sharma RK (2020) Development of wheat straw based catholyte for power generation in microbial fuel cell. *Biomass Bioenerg* 138:. <https://doi.org/10.1016/j.biombioe.2020.105591>
25. Paul D, Noori MT, Rajesh PP et al (2018) Modification of carbon felt anode with graphene oxide-zeolite composite for enhancing the performance of microbial fuel cell. *Sustain Energy Technol Assessments* 26:77–82. <https://doi.org/https://doi.org/10.1016/j.seta.2017.10.001>
26. Prabhu A, Bosakornranut E, Amraoui Y et al (2020) Enhanced xylitol production using non-detoxified xylose rich pre-hydrolysate from sugarcane bagasse by newly isolated *Pichia fermentans*. *Biotechnology for biofuels* 13:1–15. <https://doi.org/10.1186/s13068-020-01845-2>
27. Rossi R, Fedrigucci A, Setti L (2015) Characterization of electron mediated microbial fuel cell by *Saccharomyces cerevisiae*. *Chem Eng Trans* 43:337–342. <https://doi.org/10.3303/CET1543057>
28. Speranza B, Corbo MR, Campaniello D et al (2020) Biofilm formation by potentially probiotic *Saccharomyces cerevisiae* strains. *Food Microbiol* 87:. <https://doi.org/10.1016/j.fm.2019.103393>
29. Stephens K, Bentley WE (2020) Synthetic Biology for Manipulating Quorum Sensing in Microbial Consortia. *Trends Microbiol* 28:633–643. <https://doi.org/10.1016/j.tim.2020.03.009>
30. Tahir B, Mezori HA (2020) Bioethanol production from *Quercus aegilops* using *Pichia stipitis* and *Kluyveromyces marxianus*. *Biomass Convers Biorefinery*. <https://doi.org/10.1007/s13399-020-00704-2>
31. Walker G, Stewart G (2016) *Saccharomyces cerevisiae* in the Production of Fermented Beverages. *Beverages* 2:30. <https://doi.org/10.3390/beverages2040030>

32. Yuan J, Liu S, Jia L et al (2020a) Co-Generation System of Bioethanol and Electricity with Microbial Fuel Cell Technology. *Energy Fuels* 34:6414–6422. <https://doi.org/10.1021/acs.energyfuels.0c00749>
33. Yuan J, Liu S, Jia L et al (2020b) Co-Generation System of Bioethanol and Electricity with Microbial Fuel Cell Technology. *Energy Fuels* 34:6414–6422. <https://doi.org/10.1021/acs.energyfuels.0c00749>
34. Zhang Z, Cao R, Jin L et al (2019) The regulation of N-acyl-homoserine lactones (AHLs)-based quorum sensing on EPS secretion via ATP synthetic for the stability of aerobic granular sludge. *Sci Total Environ* 673:83–91. <https://doi.org/10.1016/j.scitotenv.2019.04.052>
35. Zhao Z, Zhang Y (2019) Application of ethanol-type fermentation in establishment of direct interspecies electron transfer: A practical engineering case study. *Renew Energy* 136:846–855. <https://doi.org/https://doi.org/10.1016/j.renene.2019.01.055>

## Figures

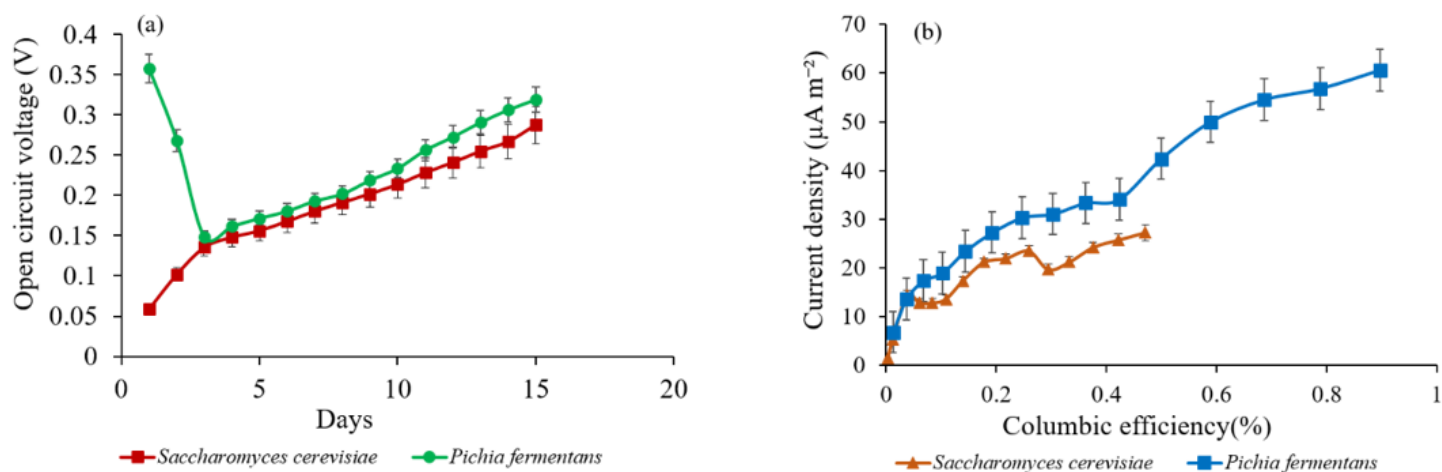
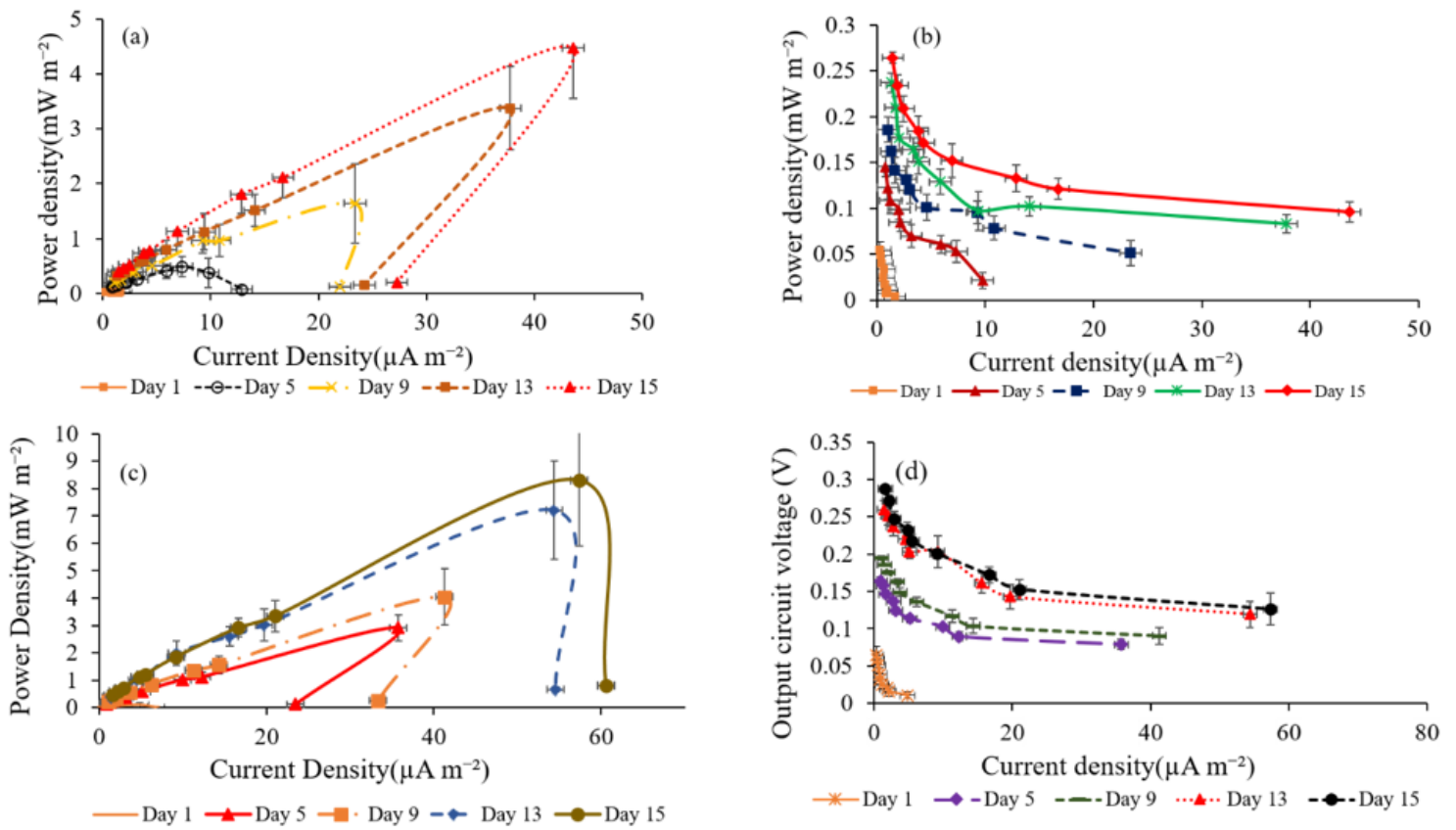


Figure 1

Open circuit voltage (a) and columbic efficiency (b) during MFC operation



**Figure 2**

Polarization curve of single chambered fuel cell with *Saccharomyces cerevisiae*; (a) Current density vs Power density and (b) Current density vs Output voltage and with *Pichia fermentans*; (c) Current density vs power density and (d) Current density vs Output voltage

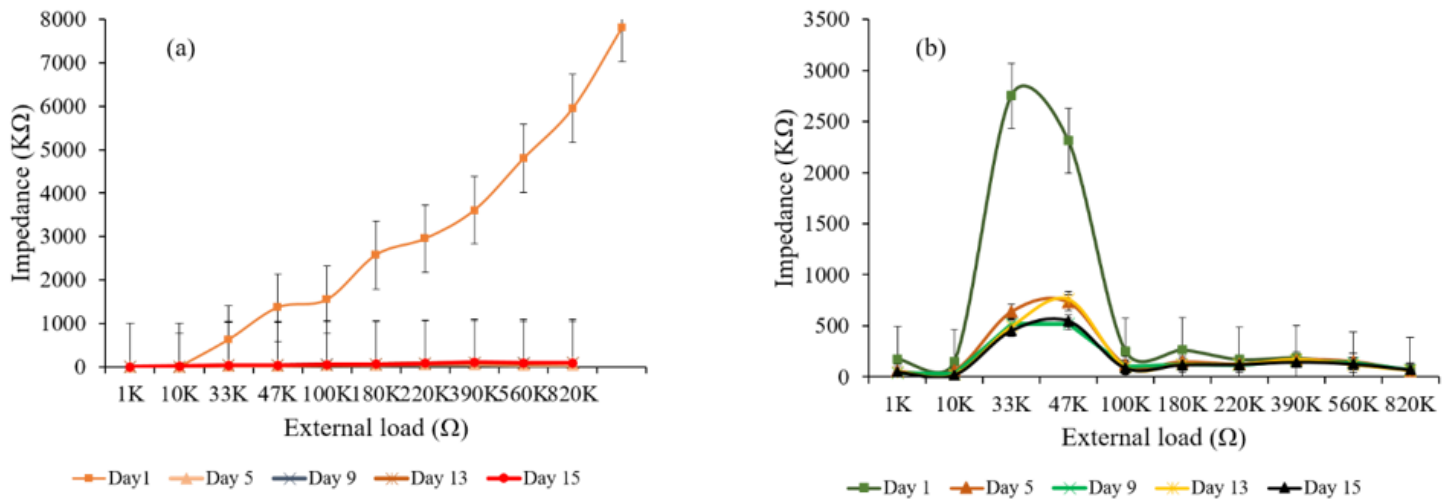


**Figure 3**

Internal resistance of *Pichia fermentans* (a) and *Saccharomyces cerevisiae* (b) at different external loads

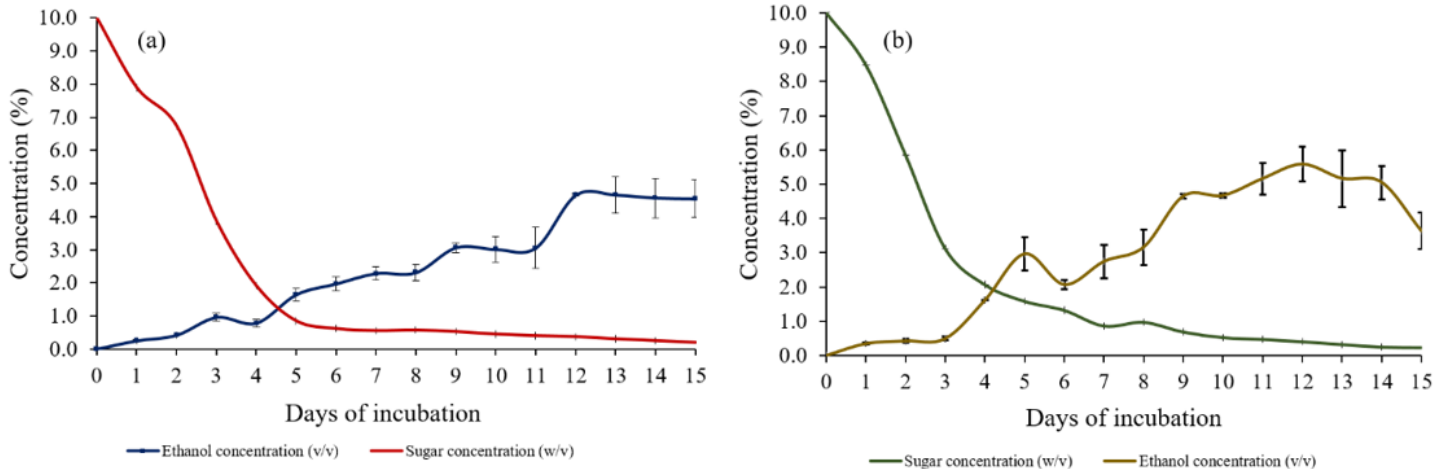


**Figure 4**

Glucose consumption and ethanol formation of (a) *Pichia fermentans* and (b) *Saccharomyces cerevisiae*

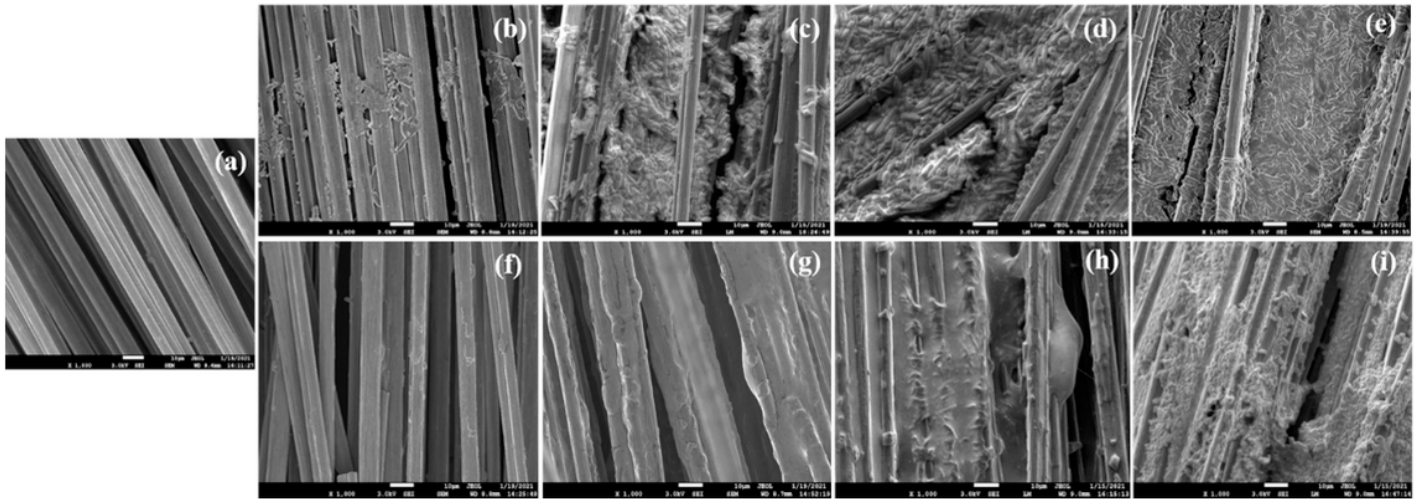


**Figure 5**

Scanning electron micrograph of biofilm formation on 10µm scale in *Pichia fermentans*; (a) carbon fibers as control with no growth, (b) after 24 h, (c) on day 5, (d) on day 10, (e) on day 15 and in *Saccharomyces cerevisiae*; (f) after 24 h, (g) on day 5, (h) on day 10, (i) on day 15

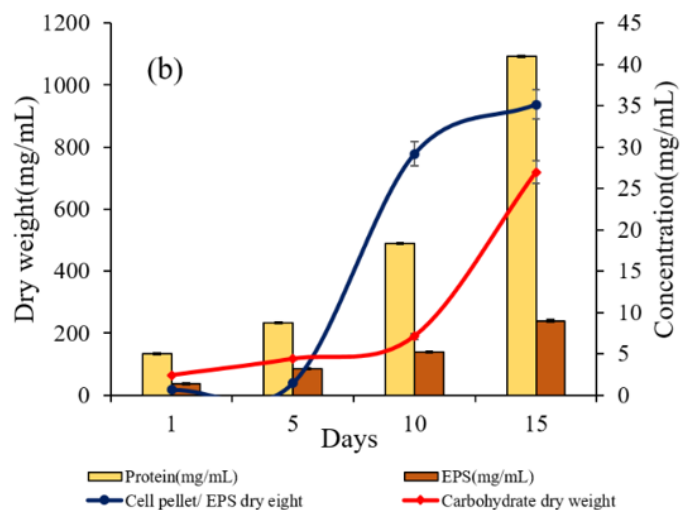
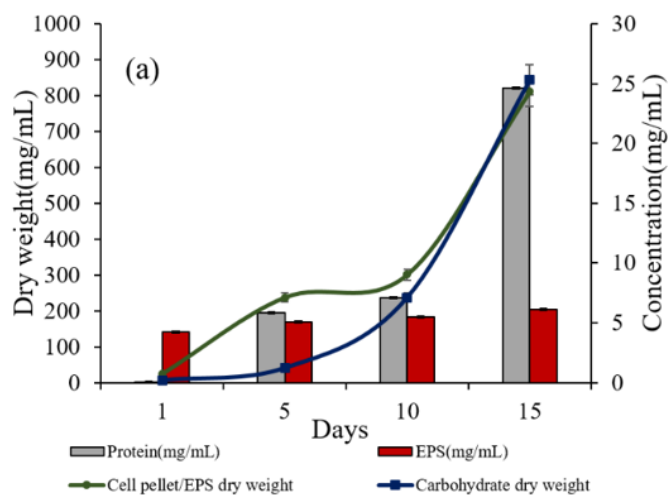


**Figure 6**

Cell biomass, EPS content and protein at different time interval for *Pichia fermentans* (a) and *Saccharomyces cerevisiae* (b)

## Supplementary Files

This is a list of supplementary files associated with this preprint. Click to download.

- [Graphicalabstract.pptx](#)
- [SupplementFigures.pptx](#)